BBA - Molecular Basis of Disease 1865 (2019) 2125–2137

Contents lists available at ScienceDirect

BBA - Molecular Basis of Disease

journal homepage: www.elsevier.com/locate/bbadis

Cardiac myocyte KLF5 regulates body weight via alteration of cardiac FGF21☆

Christine J. Pol[a], Nina M. Pollak[b,1], Michael J. Jurczak[c,2], Effimia Zacharia[a], Iordanes Karagiannides[d], Ioannis D. Kyriazis[a], Panagiotis Ntziachristos[e,3], Diego A. Scerbo[f,4], Brett R. Brown[a], Iannis Aifantis[e], Gerald I. Shulman[c], Ira J. Goldberg[f,5], Konstantinos Drosatos[a,*]

[a] Metabolic Biology Laboratory, Lewis Katz School of Medicine at Temple University, Center for Translational Medicine, Department of Pharmacology, Philadelphia, USA
[b] Institute of Molecular Biosciences, University of Graz, Graz, Austria
[c] Department of Cellular and Molecular Physiology, Yale University School of Medicine, New Haven, CT, USA
[d] Inflammatory Bowel Disease Center and Neuroendocrine Assay Core, David Geffen School of Medicine at UCLA, Los Angeles, CA, USA
[e] Howard Hughes Medical Institute, Department of Pathology, NYU School of Medicine, New York, NY, USA
[f] Division of Preventive Medicine and Nutrition, Columbia University, New York, NY 10032, USA

ARTICLE INFO

Keywords:
Krüppel-like factor
FGF21
Heart
Obesity
High fat diet

ABSTRACT

Cardiac metabolism affects systemic energetic balance. Previously, we showed that Krüppel-like factor (KLF)-5 regulates cardiomyocyte PPARα and fatty acid oxidation-related gene expression in diabetes. We surprisingly found that cardiomyocyte-specific KLF5 knockout mice (*αMHC-KLF5*$^{-/-}$) have accelerated diet-induced obesity, associated with increased white adipose tissue (WAT). Alterations in cardiac expression of the mediator complex subunit 13 (*Med13*) modulates obesity. *αMHC-KLF5*$^{-/-}$ mice had reduced cardiac *Med13* expression likely because KLF5 upregulates *Med13* expression in cardiomyocytes. We then investigated potential mechanisms that mediate cross-talk between cardiomyocytes and WAT. High fat diet-fed *αMHC-KLF5*$^{-/-}$ mice had increased levels of cardiac and plasma FGF21, while food intake, activity, plasma leptin, and natriuretic peptides expression were unchanged. Consistent with studies reporting that FGF21 signaling in WAT decreases sumoylation-driven PPARγ inactivation, *αMHC-KLF5*$^{-/-}$ mice had less SUMO-PPARγ in WAT. Increased diet-induced obesity found in *αMHC-KLF5*$^{-/-}$ mice was absent in *αMHC-[KLF5*$^{-/-}$*;FGF21*$^{-/-}$*]* double knockout mice, as well as in *αMHC-FGF21*$^{-/-}$ mice that we generated. Thus, cardiomyocyte-derived FGF21 is a component of pro-adipogenic crosstalk between heart and WAT.

1. Introduction

The heart is a central regulator of systemic metabolism as it both consumes a significant amount of fatty acids for ATP synthesis [1] and affects metabolism in other tissues, as well. Heart specific changes in lipolysis regulate circulating levels of triglycerides [2]. The heart also functions as an endocrine organ. Atrial natriuretic peptide (ANP) and brain natriuretic peptide (BNP) [3] secreted from the heart promote

Abbreviations: 18S, 18S ribosomal RNA; ANP, atrial natriuretic peptide; *Actb*, beta-actin; BNP, brain natriuretic peptide; BAT, brown adipose tissue; DIO, diet-induced obesity; FAO, fatty acid oxidation; HFD, high fat diet; KLF, Krüppel-like factor; MED13, mediator complex subunit 13; RXR, retinoid X receptor; *Rplp0*, ribosomal protein lateral stalk subunit P0; *Snord65*, small nucleolar RNA, C/D box 65; SUMO, sumoylation; WAT, white adipose tissue

☆ The authors have declared that no conflict of interest exists.

* Corresponding author at: Metabolic Biology Laboratory, Lewis Katz School of Medicine at Temple University, 3500 N. Broad Street, Philadelphia 19140, USA.
E-mail address: drosatos@temple.edu (K. Drosatos).

[1] Present address: Genecology Research Centre, School of Science and Engineering, University of the Sunshine Coast, Queensland, Australia, CSIRO Synthetic Biology Future Science Platform, Australian Institute for Bioengineering and Nanotechnology, School of Chemistry and Molecular Biosciences, University of Queensland, Queensland, Australia.

[2] Present address: Department of Medicine, Division of Endocrinology and Metabolism, University of Pittsburgh School of Medicine, Pittsburgh, PA, USA.

[3] Present address: Department of Biochemistry and Molecular Genetics and Robert H. Lurie Comprehensive Cancer Center Northwestern University, Chicago, IL, USA.

[4] Present address: Department of Biochemistry, University of Iowa Carver College of Medicine, Iowa City, IA, USA.

[5] Present address: Division of Endocrinology, Diabetes & Metabolism, NYU-Langone School of Medicine, New York, NY, USA.

https://doi.org/10.1016/j.bbadis.2019.04.010
Received 23 February 2018; Received in revised form 20 December 2018; Accepted 6 January 2019
Available online 26 April 2019
0925-4439/

lipolysis in adipose tissue [4–7]. Metabolites originating from the heart, such as phospholipase A_2, also affect systemic metabolism [8,9]. A series of studies have identified MED13 as a cardiomyocyte regulator of systemic metabolism [10,11]. Mediator complex subunit 13 (MED13) transgenic expression reduced diet-induced obesity (DIO), whereas deletion of this factor increased obesity [10,11]. MED13 is a member of the mediator complex that controls DNA transcription [12] and this gene is regulated by miR-208a [11]. How MED13 regulates systemic metabolism is unknown.

PPARγ is a central transcription factor that is essential for adipocyte development [13]. Insulin and steroids regulate PPARγ expression [14,15], and its activity is modulated by association with lipids such as certain unsaturated fatty acids and eicosanoids [16], and association with retinoid X receptor (RXR) [17]. Moreover, the activity of PPARγ can be regulated by multiple post-translational modifications, such as phosphorylation, sumoylation (SUMO), ubiquitylation, and O-GlcNAcylation [18].

FGF21, another regulator of adipose development, is mainly produced in the liver [19], but is also expressed in other tissues like white adipose tissue (WAT) [20,21], brown adipose tissue (BAT) [22,23], skeletal muscle [24,25], duodenum [23] pancreas [23,26,27], and the heart [23,28,29]. FGF21 signals primarily through the β-Klotho/FGFR1c receptor complex [30,31]. Induction of FGF21 production, as well as exogenous FGF21 administration, stimulates lipolysis in WAT [32,33], increases browning of WAT [34], and improves insulin sensitivity. Given these functions, FGF21 has been proposed as a therapeutic agent of diabetes and obesity, and increased circulating levels of FGF21 in obesity has been described as an FGF21-resistance state [35]. A recent study showed that exercise reverses diet-induced FGF21 resistance via increased adipose PPARγ activity [36]. Several studies show beneficial effects of FGF21 treatment on body weight, fat mass, and lipid and glucose metabolism of animal models and obese and diabetic patients [37–39]. On the other hand, various studies have associated greater adiposity with FGF21 expression [40,41] and have shown that FGF21 can also decrease lipolysis [42,43]. These FGF21 signaling actions in the WAT has been linked to inhibition of sumoylation of PPARγ at Lys107, resulting in increased PPARγ transcriptional activity that enhances adipogenesis [44–46]. Thus, the final positive or negative effect of FGF21 in WAT expansion and obesity seems to depend on a multifactorial signaling network that has not been fully elucidated.

Our recent study associated Krüppel-like factor (KLF)-5 with transcriptional regulation of *Ppara*, a central regulator of cardiac fatty acid oxidation (FAO) [47]. Others have shown that $KLF5^{+/-}$ mice are protected from diet-induced obesity, because of increased PPARδ-mediated energy expenditure in skeletal muscle [48]. In this report, we show that *αMHC-KLF5*$^{-/-}$ mice fed with high fat diet (HFD) had increased body weight gain compared to floxed mice on HFD, associated with reduced PPARγ sumoylation. *αMHC-KLF5*$^{-/-}$ mice had reduced cardiac *Med13* expression and we found that KLF5 is a positive regulator of *Med13* expression and causes increased heart expression of FGF21. Thus, heart production of FGF21 regulates adipose development.

2. Methods

2.1. Mouse studies

All animal studies were approved by the institutional animal care and use committees of Temple University in Philadelphia PA, Columbia University in New York NY, or Yale University in New Haven CT and mice were cared for in accordance with NIH guidelines. Mice were housed three per cage and maintained under appropriate barrier conditions in a 12hr light-dark cycle and received food and water ad libitum. The *αMHC-KLF5*$^{-/-}$ mice have been described before [47]. *αMHC-KLF5*$^{-/-}$ mice were crossed with *floxed-FGF21* mice generating mice with cardiomyocytes-specific double *Klf5* and *Fgf21* gene deletion (*αMHC-[KLF5*$^{-/-}$*;FGF21*$^{-/-}$*]*). We used 4 to 22 week old male *αMHC-KLF5*$^{-/-}$, *αMHC-[KLF5*$^{-/}$*;FGF21*$^{-/-}$*]*, or floxed (*αMHC-KLF5*$^{-/-}$ mice, which were compared with *floxed-KLF5* mice and *αMHC-[KLF5*$^{-/}$*;FGF21*$^{-/-}$*]* with floxed FGF21 or double *floxed-FGF21;KLF5* mice) mice weighing ~9–28 g. All analyses involving animals were performed with at least 3 mice per experimental group.

2.2. Cell lines

HL-1 mouse cardiac muscle cell line were maintained in Claycomb medium (Sigma-Aldrich #51800C, St. Louis, MO, USA) supplemented with 10% fetal bovine serum (Sigma-Aldrich #12103C, St. Louis, MO, USA), 100 U/ml penicillin/streptomycin (Sigma-Aldrich #P4333, St. Louis, MO, USA), 0.1 mM norepinephrine (Sigma-Aldrich #A0937, St. Louis, MO, USA), and 2 mM L-glutamine (Sigma-Aldrich #G7513, St. Louis, MO, USA) at 5% CO_2 at 37 °C [49].

2.3. Primary cardiomyocyte isolation

Adult mouse cardiomyocytes were isolated from ventricles of floxed control mice and *αMHC-FGF21*$^{-/-}$ mice as described previously [50] with minor modifications. Hearts from heparinized mice (90 USP; ip) were cannulated through the aorta. Hearts were perfused with perfusion buffer (120.4 mM NaCl, 14.7 mM KCL, 0.6 mM NaH_2PO_4, 0.6 mM KH_2PO_4, 1.2 mM $MgSO_4$, 10 mM Na-Hepes, 4.6 mM $NaHCO_3$, 30 mM taurine, 10 mM BDM, 5.5 mM glucose; pH 7.0) for 3 min followed by perfusion buffer containing 285 units/ml Collagenese type II (Worthington), 0.1–0.12 mg/ml trypsin and 0.02 mM $CaCl_2$ for 7 min. Ventricles were gently teared in small pieces, perfusion buffer containing 5 mg/ml BSA and 0.125 mM $CaCl_2$ was added and the cell suspension filtered with 100 μm nylon. The filtrate was pelleted by gravity for 5 min, centrifuged for 30 s at 0.7 rpm and the pellet resuspended in perfusion buffer containing 5 mg/ml BSA and 0.225 mM $CaCl_2$. The cells were pelleted by gravity for 10 min, centrifuged for 30 s at 0.7 rpm and the pellet resuspended in perfusion buffer containing 5 mg/ml BSA and 0.525 mM $CaCl_2$. The cells were pelleted by gravity for 10 min, centrifuged for 30 s at 0.7 rpm and the pellet resuspended in perfusion buffer containing 5 mg/ml BSA and 1.025 mM $CaCl_2$. The cells were pelleted by gravity for 10 min, centrifuged for 30 s at 0.7 rpm and the pellet resuspended in TRIzol reagent (Invitrogen) for RNA isolation.

2.4. High fat diet treatment

αMHC-KLF5$^{-/-}$, *αMHC-[KLF5*$^{-/}$*;FGF21*$^{-/-}$*]*, or floxed mice were fed HFD (60 kcal% fat, D12492i; Open Source Diet) starting when mice were 4 to 23 weeks old. Mice were sacrificed after 6 to 8 weeks HFD following anesthesia with isoflurane inhalation. Blood was collected, mice were perfused with PBS via the apex, and heart, posterior subcutaneous WAT, BAT, kidney, skeletal muscle, and liver were harvested. Heart, WAT, BAT, kidney, skeletal muscle, and liver samples were flash frozen and WAT, BAT, and liver samples were put in tissue tek, and stored at −80 °C until further use.

2.5. Metabolic cages analysis

In a subset of HFD-fed *αMHC-KLF5*$^{-/-}$ and floxed mice major determinants of energy balance, including feeding, activity, energy expenditure by indirect calorimetry and drinking, were measured using the Columbus Labs Comprehensive Lab Animal Monitoring System (CLAMS) [51]. Mice were individually housed for three to four days prior to metabolic cage study and acclimated within the cages for an additional 24 h. Data were collected for 48 h and are reported as the 24-hour average per mouse.

2.6. RNA purification and gene expression analysis

Total RNA was purified from hearts, WAT, BAT, skeletal muscle, kidney, and liver using the TRIzol reagent according to the instructions of the manufacturer (Invitrogen). DNase-treated (Invitrogen) RNA was used for cDNA synthesis using the Protoscript II First-Strand cDNA Synthesis kit (New England BioLabs). cDNA was analyzed with quantitative real-time PCR that was performed with SYBR Select Master Mix (Applied Biosystems). qRT-PCR was performed on an Applied Biosystems StepOnePlus Real-Time PCR system. Samples were normalized against 18S ribosomal RNA (*18S*), ribosomal protein lateral stalk subunit P0 (*Rplp0*/36B4), or beta-actin (*Actb*). The BioRad Fgf21 primer assay (10025636) was used for *Fgf21* detection. The sequences of the other primers have been described previously [47,52], or are described in Table S1. Expression levels of miR-208 was analyzed using a microRNA PCR kit (Exiqon) and samples were normalized against 5S ribosomal RNA (*5S*), small nucleolar ribonucleoprotein *U6* and small nucleolar RNA, C/D box 65 (*Snord65*).

2.7. Plasma FGF21, adiponectin, leptin, triglyceride, and glucose levels

Plasma and liver TG levels were measured using Infinity Triglyceride Reagent (Thermo Scientific) according to the manufacturer's instructions. Glucose levels were measured in plasma using a blood glucose meter (Contour next; Bayer). ELISA kits were used to measure plasma levels of leptin (EZML-82K; EMD Millipore), adiponectin (EZMADP-60K; EMD Millipore), BNP (EIAM-BNP; RayBio), and FGF-21 (MF2100; R&D systems) according to the manufacturer's instructions.

2.8. Protein and post-translational modifications analysis

IP: Total protein was isolated from whole fat tissue after grinding in 300 µl of RIPA buffer. Supernatants were collected and placed in fresh tubes where protein concentration was determined via Bradford assay (BCA Protein Assay kit, Fisher). 4 µl of Anti-PPARγ antibody (D69, Cell Signaling) were then added to 200 µg the total protein supernatants with a final concentration of 1 mg/ml and incubated O/N with rotation at 4 °C. Then, we added 30 µl of Protein A agarose beads (Cell Signaling, #9863) to each sample and incubated at 4 °C for 3 h. The samples were then microcentrifuged for 30 s at 4 °C and washed 5× using 500 µl 1× RIPA buffer. Pellets were then re-suspended in 40 µl 6× SDS-sample buffer (Boston Bioproducts) denatured by boiling and used for western immunoblotting. Western Blotting: Proteins were separated by electrophoresis in a 10% polyacrylamide gel. Samples were electrophoresed at 100–150 V for 1.5 h and the separating gel was equilibrated in transfer buffer (20 mm Tris-HCl, 150 mm glycine, 20% methanol, and 0.1% sodium dodecyl sulfate) for 10 min. The proteins were then transferred to Immobilon-FL membranes (Millipore, Billerica, MA) at 4 °C, O/N. The membranes were then blocked for 1 h at room temperature in protein-free (PBS) blocking buffer (Pierce) and incubated at a 1:1000 dilution with a mouse primary antibody against SUMOylated proteins (SUMO-1 2A12, Cell Signaling, # 5718 in blocking buffer, O/N at 4 °C. The membrane was then blotted with the IRDye® 800CW Goat anti-Mouse IgG secondary antibody 1:15,000 (LI-COR) in blocking buffer for 1 h and the proteins were visualized and quantified using the Odyssey CLx Imaging system (LI-COR).

2.9. Histology

Cryosections of WAT and BAT were stained with H&E staining and cryosections of liver were stained with Oil Red O staining by the immunohistochemistry core at NYU, New York. Of each section up to up to 10 pictures were taken randomly at 10× or 20× magnification. WAT adipocyte size in *αMHC-KLF5* or floxed mice was measured in images of 10× magnification in all cells (at least 93 cells per mouse) using ImageJ software. WAT adipocyte size in *αMHC-[KLF5*$^{-/-}$*;FGF21*$^{-/-}$*]* or floxed mice was measured in images of 20× magnification in all cells (at least 28 cells per mouse) using ImageJ software.

2.10. Adenoviral infection

The recombinant adenovirus that expresses KLF5 was kindly provided by Dr. Ceshi Chen [53]. HL-1 cells were infected with ad-KLF5 or control adenovirus-expressing GFP (Ad-GFP) at a multiplicity of infection (MOI) of 10 in medium supplemented with 2% Heat-Inactivated Horse Serum and 1% Penicillin/Streptomycin for 6 h. The medium was then replaced with 10% FBS-containing medium and cells were harvested after an additional 48 h [49].

2.11. Chromatin immunoprecipitation (ChIP)

HL-1 cells were subjected to ChIP as previously described [54]. The antibodies used for ChIP were anti-KLF5 (07-1580; Millipore), and anti-IgG. Precipitated DNA was further analyzed with RT PCR.

2.12. Statistics

Data are expressed as the mean ± SEM. Western Blots are quantified using the Odyssey CLx Imaging system (LI-COR). Statistical significance was assessed using GraphPad Prism 6 software with the appropriate test; 2 tailed *t*-test, 1-way ANOVA, or 2-way ANOVA followed by Tukey's multiple comparisons test. A $P < 0.05$ was considered statistically significant. The values of n, statistical measures (mean ± SEM), and statistical significance are reported in the figures and figure legends.

3. Results

3.1. Cardiomyocyte-specific KLF5 deletion accelerates DIO

We previously showed that cardiomyocyte KLF5 is a positive transcriptional regulator of *Ppara*, as well as that KLF5 inhibition decreases FAO and eventually leads to cardiac dysfunction [47]. As previous studies have correlated inhibition of cardiac fatty acid utilization with altered systemic lipid metabolism [55], we treated *αMHC-KLF5*$^{-/-}$ mice with HFD for 6 weeks. Surprisingly, *αMHC-KLF5*$^{-/-}$ mice showed accelerated DIO (Fig. 1A and B), compared to HFD-fed control floxed

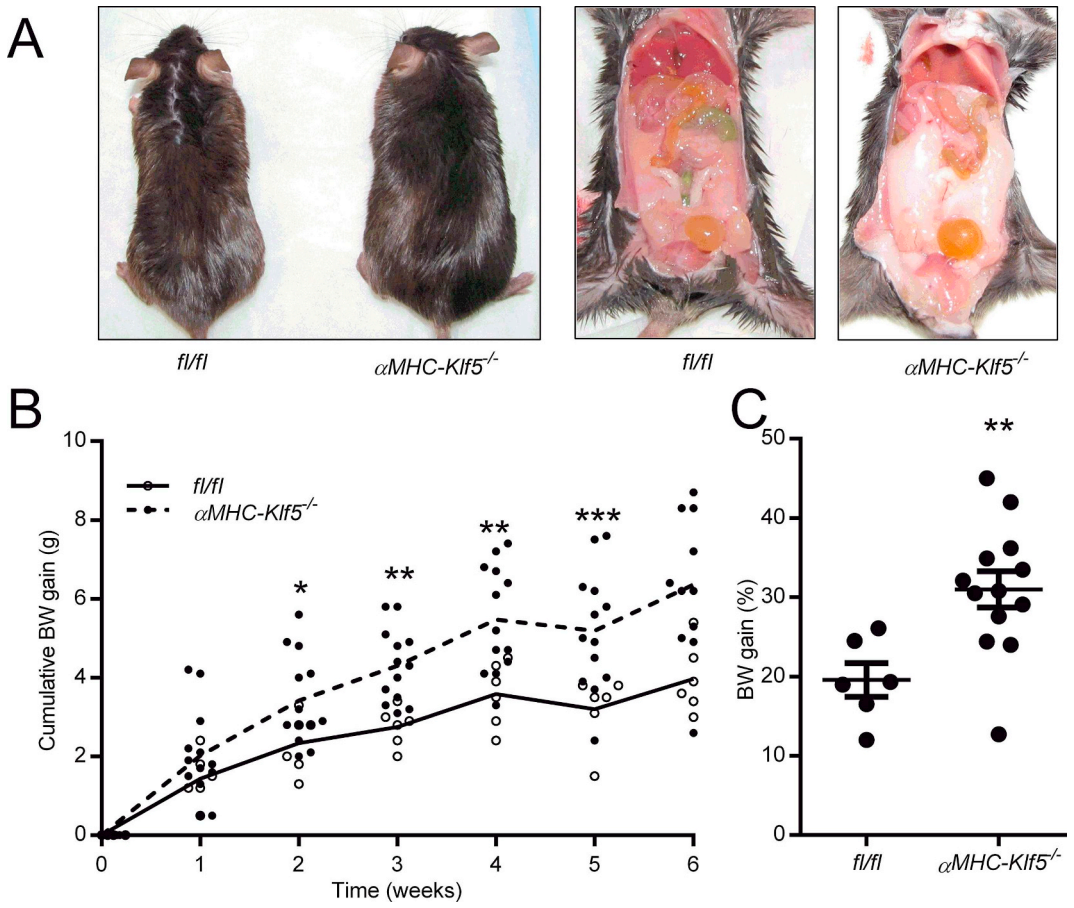

Fig. 1. Cardiomyocyte-specific KLF5 deletion accelerates diet-induced obesity – A: Representative pictures of control floxed or *αMHC-KLF5*$^{-/-}$ mice after 6 weeks of HFD. B–C: Cumulative body weight gain (g) (B), body weight gain (%) (C) of control floxed (n = 6) and *αMHC-KLF5*$^{-/-}$ (n = 13) mice after 6 weeks HFD (*$p < 0.05$, **$p < 0.01$, ***$p < 0.001$ vs floxed with 2way ANOVA (B) or Student's *t*-test (C)). Data are presented as mean ± SEM. (See also Fig. S1A–D) HFD: high fat diet, KLF: Krüppel-like factor.

mice. The percentage of body weight gain over 6 weeks of HFD-fed *αMHC-KLF5*$^{-/-}$ mice was 1.55 times greater than HFD-fed control floxed mice (20% vs 31%) (Fig. 1C). The increased body weight gain was associated with a trend ($p = 0.12$) for increased WAT weight (Fig. 2A), and increased mRNA levels of proteins that are positively correlated with adipocyte lipid metabolism: *Pparg1*, *Pparg2*, lipoprotein lipase (*Lpl*), *Cd36*, diacylglycerol o-acyltransferase 2 (*Dgat2*), and glucose transporter 4 (*Glut4*) (Fig. 2B). Histological analysis (H&E staining) of WAT and BAT showed larger adipocytes in WAT and more lipid accumulation in BAT obtained from HFD-fed *αMHC-KLF5*$^{-/-}$ mice (Figs. 2C and S1A). Also, Oil-Red-O staining and biochemical analysis indicated increased hepatic triglyceride (TG) content in HFD-fed *αMHC-KLF5*$^{-/-}$ mice (Figs. 2D and S1B). Plasma TG and glucose levels were similar in HFD-fed wild type mice and HFD-fed *αMHC-KLF5*$^{-/-}$ mice (Fig. S1C and D).

We next evaluated the food intake and activity levels of the mice as a possible explanation of the difference in weight gain. Metabolic cage analysis did not show significant differences in respiratory exchange ratio, caloric intake, activity, and energy expenditure between HFD-fed *αMHC-KLF5*$^{-/-}$ and control floxed mice fed with HFD (Fig. 3A–D). Thus, the differences in these parameters were not great enough to detect with this method.

3.2. KLF5 is a miR-208-independent, direct positive regulator of cardiac MED13

As the effect of cardiomyocyte-specific deletion of KLF5 in the expansion of WAT resembles the phenotype of HFD-fed *αMHC-MED13*$^{-/-}$ mice [11], we assessed whether KLF5 regulates *Med13* expression. The *αMHC-KLF5*$^{-/-}$ mice have reduced cardiac *Med13* mRNA levels (Fig. 4A), which may account for DIO. However, miR-208, which targets *Med13* transcript [11], was not increased, on the contrary it showed a trend ($p = 0.29$ for male mice and $p = 0.13$ for female mice) to decrease (Fig. 4B). Then, we treated HL-1 cells with adenovirus expressing KLF5 (ad-KLF5) or GFP (ad-GFP) as control. Overexpression of KLF5 significantly increased *Med13* expression (Fig. 4C). Furthermore, in silico promoter analysis (Genomatix software) followed by alignment (CLUSTAL O - 1.2.0) of mouse and human *Med13* promoters (obtained from the UCSC Genome Browser) identified two potential KLF5 binding sites in the −730/−713 bp region and in the −142/−125 bp region (Fig. 4D). Chromatin immunoprecipitation in HL-1 cells treated with ad-KLF5 showed enrichment of the −730/−713 bp region (Fig. 4E) but

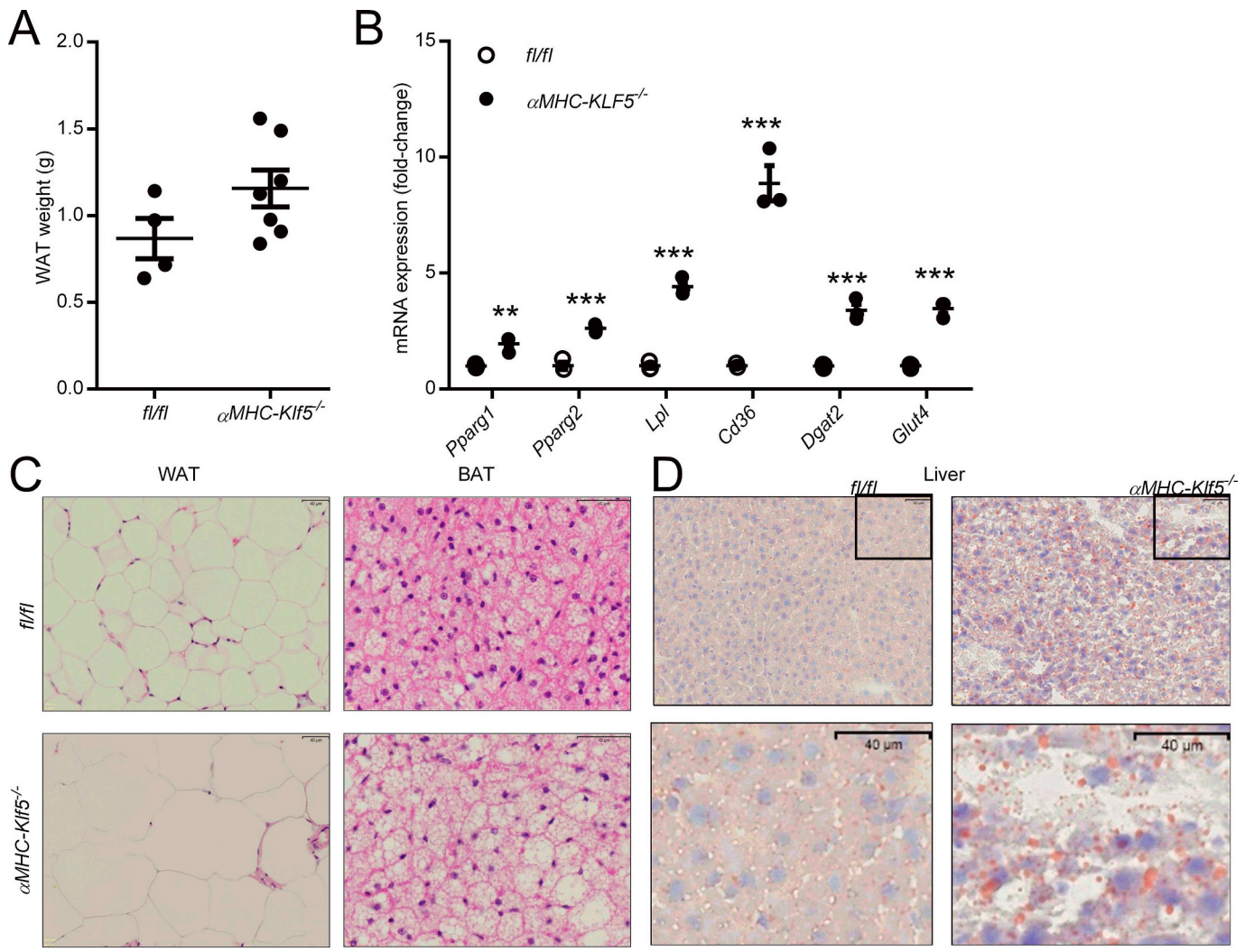

Fig. 2. Cardiomyocyte-specific KLF5 deletion promotes adipose tissue expansion and hepatic lipid accumulation – A: posterior subcutaneous WAT weight of control floxed (n = 4) and *αMHC-KLF5*$^{-/-}$ (n = 7) mice after 6 weeks HFD. B: mRNA levels of lipid metabolism markers *Pparg1*, *Pparg2*, *Lpl*, *Cd36*, *Dgat2* and *Glut4* in WAT isolated from control floxed or *αMHC-KLF5*$^{-/-}$ mice after 6 weeks of HFD (n = 3; **p < 0.01, ***p < 0.001 with Student's *t*-test). C–D: Representative pictures of H&E staining of WAT and BAT (C), and Oil Red O staining of liver (D) of control floxed and *αMHC-KLF5*$^{-/-}$ mice after 6 weeks HFD. Data are presented as mean ± SEM. BAT: brown adipose tissue, Dgat: diglyceride acyltransferase, Glut: glucose transporter, HFD: high fat diet, KLF: Krüppel-like factor, Lpl: lipoprotein lipase, WAT: white adipose tissue.

not the −142/−125 bp region (Fig. 4F) of *Med13* promoter with KLF5. Thus, KLF5 is a positive regulator of *Med13* gene expression.

3.3. *αMHC-KLF5*$^{-/-}$ mice on HFD have increased FGF21 signaling

We then investigated what mechanism may underlie the cross-talk between cardiomyocytes and WAT expansion. Plasma leptin and adiponectin levels are not changed in HFD-fed *αMHC-KLF5*$^{-/-}$ mice compared to control HFD-fed floxed mice (Fig. 5A and B). We then assessed the cardiac endocrine factors ANP and BNP that have lipolytic properties in adipose tissue [4,56], and are inversely associated with obesity [57–59]. We have previously shown that cardiac *Bnp* expression is increased in chow *αMHC-KLF5*$^{-/-}$ mice compared to floxed mice [47], and here we show that HFD-fed *αMHC-KLF5*$^{-/-}$ mice have increased cardiac *Bnp* expression compared to HFD-fed floxed mice (Fig. 5C). Plasma BNP levels were not increased in HFD-fed *αMHC-KLF5*$^{-/-}$ mice (Fig. 5D). Accordingly, cardiac *Anp* expression levels were increased in HFD-fed *αMHC-KLF5*$^{-/-}$ mice (Fig. 5C).

Based on observations that have associated FGF21 with fat content either in a positive [37–39] or negative way [40,41], we measured cardiac gene expression and plasma FGF21 levels, which were increased in HFD-fed *αMHC-KLF5*$^{-/-}$ mice (Fig. 6A and B). Accordingly, mRNA levels of *Fgfr* and Klotb that transmit FGF21 signaling were increased in WAT obtained from HFD-fed *αMHC-KLF5*$^{-/-}$ mice (Fig. 6C). Increased FGF21 signaling has been associated with inhibition of PPARγ SUMOylation [44]. To assess sumoylation of PPARγ, we

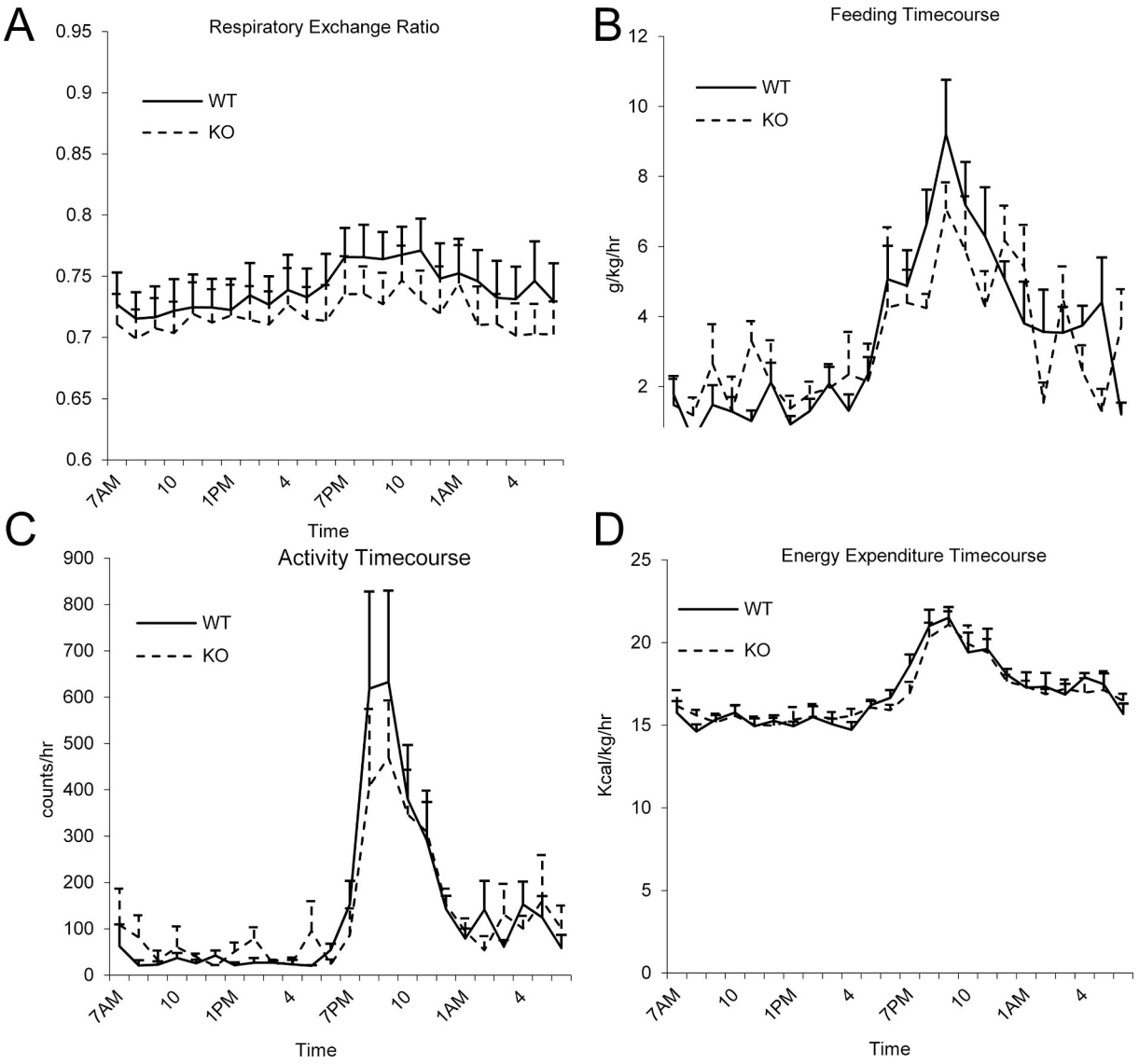

Fig. 3. Cardiomyocyte-specific KLF5 deletion does not alter significantly respiratory exchange ratio, caloric intake, activity, and energy expenditure at the early stage of HFD – Respiratory exchange ratio (A), feeding time course (B), activity time course (C), and energy expenditure (D) from metabolic cage analysis of control floxed (n = 6) and *αMHC-KLF5*$^{-/-}$ (n = 5) mice on HFD for 3 weeks. Data are presented as mean ± SEM. HFD: high fat diet, KLF: Krüppel-like factor.

immunoprecipitated PPARγ from WAT protein and then performed western blots with pan-SUMO antibody. WAT of HFD-fed *αMHC-KLF5*$^{-/-}$ mice showed decreased sumo-PPARγ to total PPARγ ratio (Fig. 6D). The expression of SUMO-specific proteases (SENPs), which may regulate sumoylation and desumoylation was not altered in WAT of *αMHC-KLF5*$^{-/-}$ mice on HFD (Fig. S2).

3.4. FGF21 mediates increased weight gain of αMHC-KLF5$^{-/-}$ mice on HFD

In order to assess whether cardiomyocyte-derived FGF21 has a distinct effect in mediating the obesogenic effect of *Klf5* ablation, we generated mice with cardiomyocyte-specific double knockout of *Klf5* and *Fgf21* (*αMHC-[KLF5*$^{-/-}$*;FGF21*$^{-/-}$*]*) and fed them with HFD. The *αMHC-[KLF5*$^{-/-}$*;FGF21*$^{-/-}$*]* mice have reduced cardiac *Fgf21* mRNA levels by 95% (Fig. 7A). When these mice were fed with HFD, they did not show increased body weight gain (Fig. 7B and C), or WAT weight (Fig. 7D) compared to control floxed mice on HFD. Plasma FGF21 levels in HFD-fed *αMHC-[KLF5*$^{-/-}$*;FGF21*$^{-/-}$*]* mice were decreased compared to control floxed mice on HFD (Fig. 7E). The double cardiomyocyte-specific knockout of *Klf5* and *Fgf21* also prevented the increased expression of lipid metabolism-related gene expression markers in WAT (Figs. 7F, 1A), the increase in adipocyte size in WAT, and the increased lipid accumulation in BAT and liver that was found in *αMHC-KLF5*$^{-/-}$ mice on HFD (Figs. 8A, B, 2C, D, S1E). Plasma TG levels were normal and glucose levels are slightly decreased (15%) in *αMHC-*

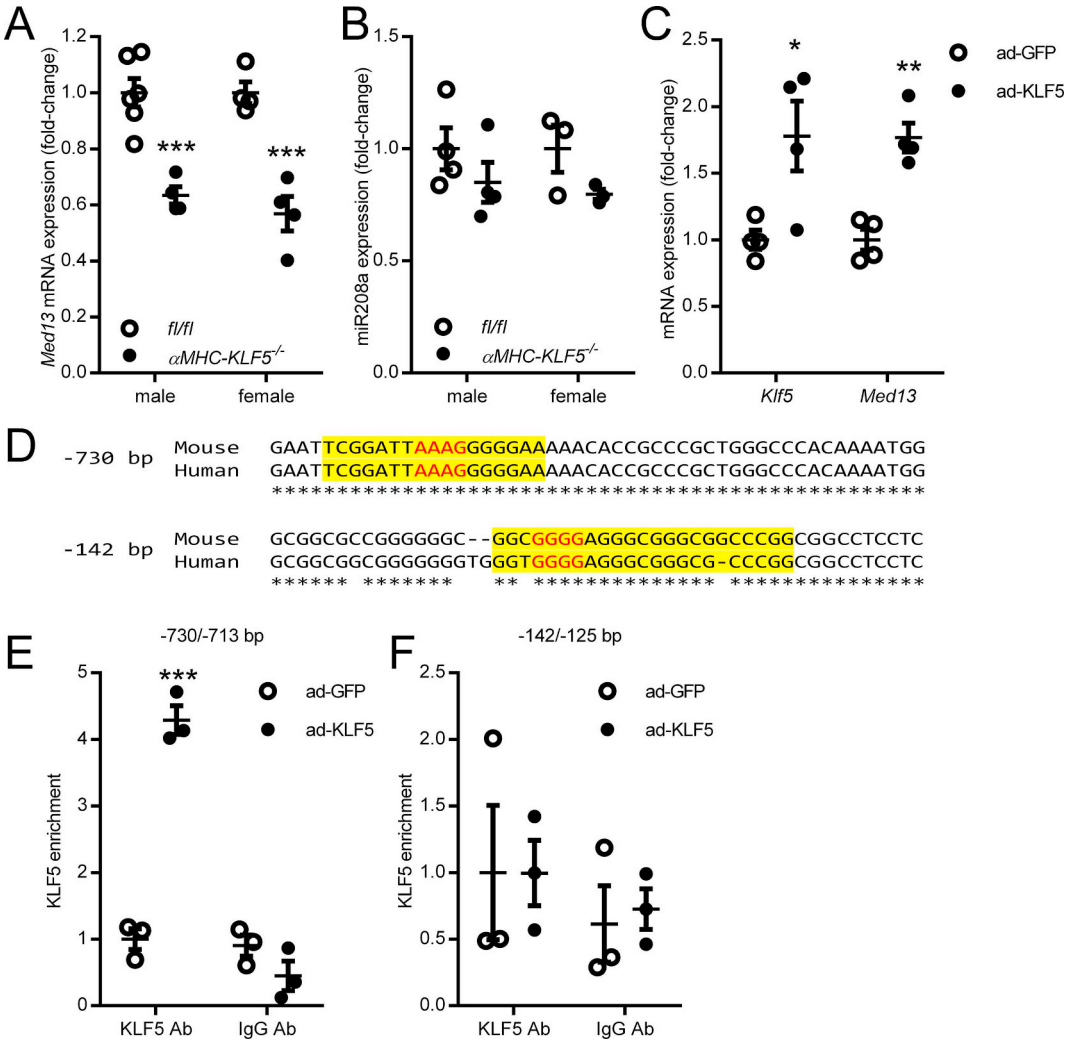

Fig. 4. KLF5 is a miR-208-independent, direct positive regulator of cardiac MED13 – A–B: Cardiac *Med13* mRNA levels (n = 4–6; ***$p < 0.001$ with Student's *t*-test) (A) and miR-208a levels (n = 3–4) (B) in male and female control floxed and *αMHC-KLF5*$^{-/-}$ mice. C: *Klf5* and *Med13* mRNA levels in HL-1 cells treated with Ad-GFP or Ad-KLF5 (n = 4, *$p < 0.05$; **$p < 0.01$ vs ad-GFP with Student's *t*-test). D: Predicted KLF-binding sites by in silico promoter analysis on aligned mouse and human *Med13* promoters (highlighted in yellow). E–F: Enrichment of −730/−713 bp region (E) or −142/−125 bp region (F) (highlighted in yellow) of mouse *Med13* promoter with KLF5 of chromatin samples from HL-1 cells treated with Ad-GFP or Ad-KLF5 (n = 3; ***p < 0.001 vs Ad-GFP with Student's *t*-test). Data are presented as mean ± SEM. Ad: adenovirus, KLF: Krüppel-like factor, Med13: mediator complex subunit 13.

[KLF5$^{-/-}$*;FGF21*$^{-/-}$*]* mice on HFD compared to control floxed mice on HFD (Fig. S1F and G). HFD-fed *αMHC-[KLF5*$^{-/-}$*;FGF21*$^{-/-}$*]* mice had no change in PPARγ sumoylation in WAT (Fig. 8C). Cardiac *Med13* expression was still lower in HFD-fed *αMHC-[KLF5*$^{-/-}$*;FGF21*$^{-/-}$*]* than control floxed mice (Fig. 8D). Thus, cardiomyocyte-specific deletion of *Fgf21* prevents accelerated DIO driven by cardiac *Klf5* ablation despite downregulation of MED13, although downregulation of *Med13* expression in *αMHC-[KLF5−/−;FGF21−/−]* male mice seems to be less robust (−25%) than the respective change in *αMHC-KLF5−/−* mice of the same gender (−35%).

To further assess the potential role of cardiomyocyte-derived FGF21 in DIO, independent from KLF5, we generated mice with cardiomyocyte-specific *Fgf21* deletion (*αMHC-FGF21*$^{-/-}$). These mice have decreased FGF21 expression (70%) in isolated cardiomyocytes (Fig. S3A). Treatment of *αMHC-FGF21*$^{-/-}$ mice with HFD did not change the cumulative body weight gain compared to control floxed mice on HFD, but the relative (%) body weight gain was decreased (Fig. S3B and C). Thus, the body weight gain of the *αMHC-FGF21*$^{-/-}$ mice on HFD was lower compared to HFD-fed control floxed mice. Plasma FGF21 levels in HFD-fed *αMHC-FGF21*$^{-/-}$ mice were not changed (Fig. S3D). *Fgf21* mRNA expression in liver, skeletal muscle, WAT, BAT, and kidney were similar between control floxed, *αMHC-KLF5*$^{-/-}$, *αMHC-FGF21*$^{-/-}$, and *αMHC-[KLF5*$^{-/-}$*;FGF21*$^{-/-}$*]* mice on HFD (Fig. S3E), suggesting that FGF21 derived from other tissues does not contribute to

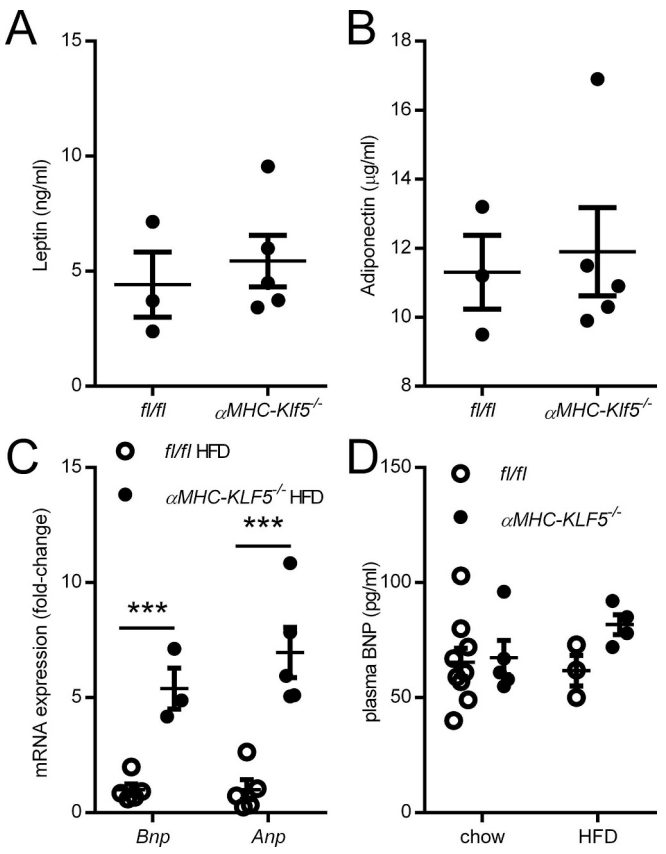

Fig. 5. *αMHC-KLF5*$^{-/-}$ mice on HFD have neither higher leptin and adiponectin nor lower natriuretic peptide levels – A–B: Leptin (A) and adiponectin (B) levels in plasma obtained from control floxed and *αMHC-KLF5*$^{-/-}$ *mice* after 6 weeks of HFD (n = 3–5). C: Cardiac *Anp* and *Bnp* mRNA expression from control floxed and *αMHC-KLF5*$^{-/-}$ *mice* after 6 weeks HFD diet (n = 3–5, ***p < 0.001 with Student's *t*-test). D: BNP levels in plasma from control floxed and *αMHC-KLF5*$^{-/-}$ *mice* after 6 weeks in HFD (n = 3–9). Data are presented as mean ± SEM. ANP; atrial natriuretic peptide, BNP: brain natriuretic peptide, HFD: high fat diet, KLF: Krüppel-like factor. (See also Fig. S3).

the changes in plasma FGF21 levels between the different strains.

4. Discussion

Various organs, such as the heart, liver [60], skeletal muscle [24,61], bones [62] and gut microbiota [63] affect WAT expansion. Specifically, skeletal muscle [64,65], gut [66], bone [62], liver [60,67], and the heart [4–7,10,11,68,69] secrete factors that affect systemic lipid metabolism and adipose tissue. A previous study has shown that reduced cardiac *Med13* accelerates DIO and overexpression of this gene reduces DIO [10,11]. The reasons for this are unknown but suggest that *Med13* regulates production of a secreted factor that affect adipose biology. Parabiosis experiments are consistent with this conclusion [10]. We found that KLF5 is a positive regulator of *Med13* expression.

Here, we show that cardiomyocyte *Klf5* ablation increases body weight gain rate, as well as that this effect of cardiomyocyte KLF5 is abrogated upon deletion of cardiomyocyte-derived FGF21. Increased plasma FGF21 levels that are observed in *αMHC-KLF5*$^{-/-}$ mice result in PPARγ activation in WAT causing increased adiposity. This is the first time an endocrine action of cardiomyocyte-derived FGF21 is demonstrated. The cardiac KLF5-FGF21 signaling pathway found in this study might play a role in diabetes as we have previously shown in diabetic animal models of both insulin-deficient and Type 2 diabetes that Klf5 expression is downregulated at the early stage of diabetes and increased as the disease progresses [47]. In this previous study we also showed that KLF5 is a positive regulator of *Ppara* gene transcription. Others have shown that cardiac specific PPARα overexpression leads to hepatic insulin resistance and future studies will need to show whether cardiac KLF5-mediated changes in PPARα signaling and altered insulin sensitivity in other tissues contribute towards the DIO of αMHC-KLF5−/− mice [70]. Interestingly, in both αMHC-Klf5$^{-/-}$ and the *αMHC-[KLF5*$^{-/-}$*;FGF21*$^{-/-}$*]* mice, we observed a small trend for reduced plasma glucose levels.

HFD-fed *αMHC-[KLF5*$^{-/-}$*;FGF21*$^{-/-}$*]* mice also have lower cardiac *Med13* mRNA levels compared to HFD-fed control floxed mice (Fig. 8D) but normal body weight gain rate. Whether *αMHC-KLF5*$^{-/-}$ mice on HFD also have a cardiac phenotype and develop cardiomyopathy will be subject of future study. The interrelationship between cardiomyocyte *Med13* and *Fgf21* expression, as well as whether cardiomyocyte-derived FGF21 may be involved in the induction of the obesogenic phenotype of *αMHC-MED13*$^{-/-}$ mice remains to be investigated [10]. But our data suggest that not all sources of FGF21 have identical actions, and that cardiac FGF21 works different from hepatic FGF21.

In our study the increased cardiac FGF21 expression levels in HFD-fed *αMHC-KLF5*$^{-/-}$ mice are associated with increased plasma levels of FGF21. Although plasma FGF21 is not decreased in *αMHC-FGF21*$^{-/-}$ mice, which may be due to compensatory FGF21 production from other tissues or due to the limits of detection sensitivity, plasma FGF21 levels are decreased in *αMHC-[KLF5*$^{-/-}$*;FGF21*$^{-/-}$*]* mice. Cardiomyocyte-specific overexpression of FGF21 has been shown to increase circulating levels of FGF21 and a moderate decreased body weight due to a reduction in lean body mass while fat mass was increased [41]. Although increased circulating levels of FGF21 during obesity, fasting, and refeeding have been shown to originate from the liver [71], mitochondrial dysfunction and stress increase cardiac and circulating levels of FGF21 without an increase in hepatic FGF21 levels [72].

The role of FGF21 in regulating body weight has been controversial and it seems to rely on the source of FGF21, as well as on acute or chronic administration. Previous reports have associated FGF21 with anti-diabetic and weight-lowering effects [37,38]. Various studies have demonstrated beneficial metabolic effects of systemic administration of exogenous FGF21, and reduction of body weight and plasma lipid and glucose levels in obesity [37,38,73–76]. Adipose tissue-specific constitutive expression of the FGF21 co-receptor, β-Klotho, in mice that underwent exogenous administration of human FGF21 also lowered body weight gain rate compared to HFD-fed control mice [77]. In addition, treatment of obese non-human primates and obese and diabetic patients with FGF21 mimetics show beneficial effects on lipid profile and body weight [39,78]. Chronic treatment of HFD-fed mice with FGF21 decreased body weight, fat mass, and liver steatosis [79]. *Fgf21*$^{-/-}$ mice have increased body weight and fat mass on normal chow or ketogenic diet, but similar body weight as wild type mice on HFD [26,35,80]. A recent study using tissue specific β-klotho KO mice shows that the body-lowering effect of FGF21 administration on weight loss is mediated primarily by the central nervous system [81]. Other effects of FGF21 to reduce glucose and lipid levels are found with

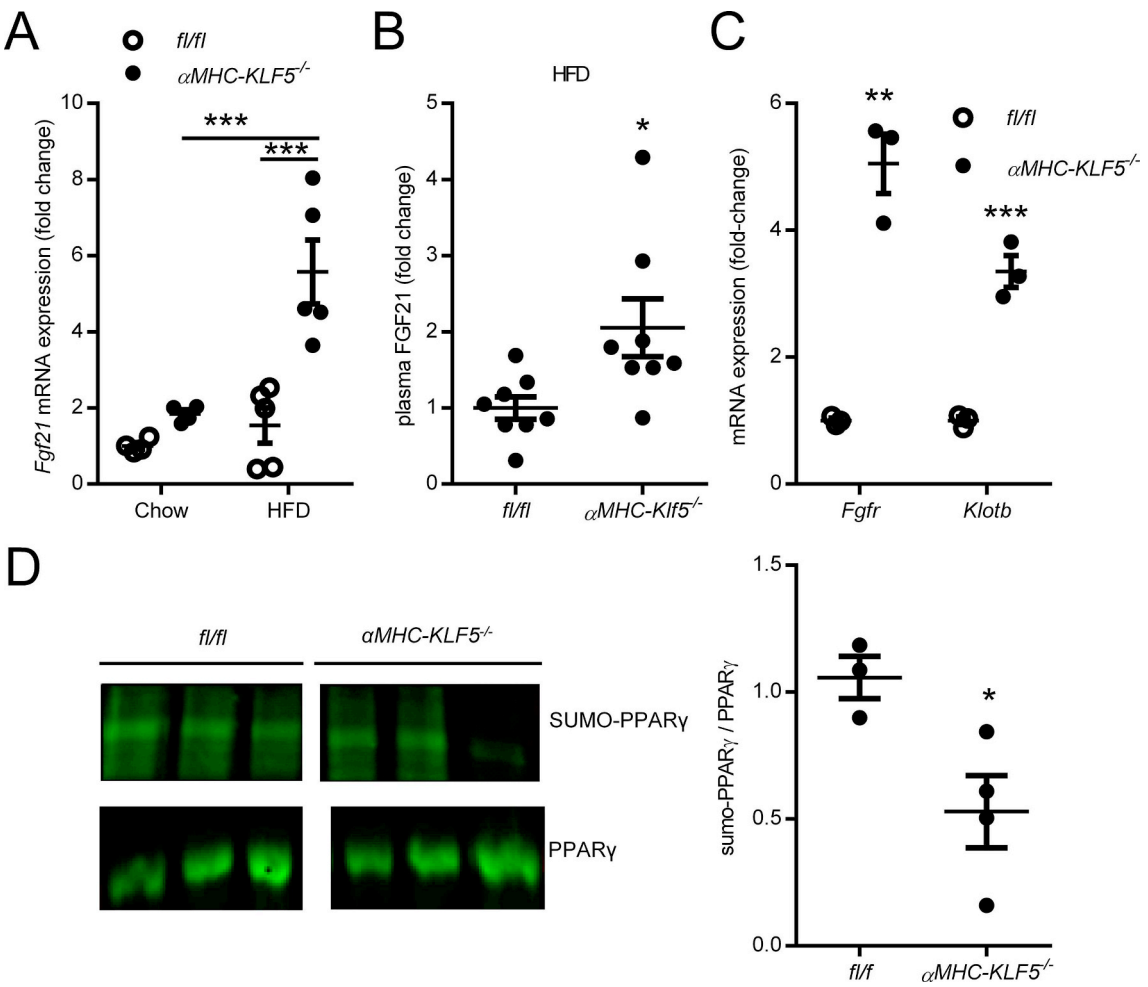

Fig. 6. *αMHC-KLF5*$^{-/-}$ mice on HFD have increased FGF21 signaling – A–D: Cardiac *Fgf21* mRNA expression (n = 4–5, ***p < 0.001 with 2way ANOVA) (A), and plasma FGF21 levels (n = 8, *$p < 0.05$ with Student's *t*-test; 95% CI 69.7–138.9 pg/ml in control floxed and 118.7–233.5 pg/ml in *αMHC-KLF5*$^{-/-}$ mice) (B) in control floxed and *αMHC-KLF5*$^{-/-}$ mice after 6 weeks in HFD. C: *Fgf21r* and *Klotb* mRNA levels in WAT obtained from control floxed and *αMHC-KLF5*$^{-/-}$ mice after 6 weeks in HFD (n = 3, **p < 0.01, ***p < 0.001 vs floxed with Student's *t*-test). D: Representative western blot image and quantitative analysis of sumo-PPARγ and PPARγ protein levels obtained with immunoprecipitation from WAT isolated from control floxed and *αMHC-KLF5*$^{-/-}$ mice after 6 weeks in HFD (n = 3–4, *$p < 0.05$ with Student's *t*-test). The lanes were run on the same gel but were noncontiguous. Data are presented as mean ± SEM. HFD: high fat diet, KLF: Krüppel-like factor.

exogenous administration or transgenic overexpression and 5-fold or higher increases of FGF21 levels [41,75], which are much greater than those found in our mice. In contrast to these findings, FGF21 signaling in adipose tissue improves insulin-sensitivity [71]. Insulin drives pre-adipose differentiation and greater adipose mass [82]. FGF21 decreases lipolysis in human adipocytes in vitro (Fig. 1A in [42]) and in mouse primary adipocytes (Fig. 2B in [43]). Cardiomyocyte-specific over-expression of FGF21 has been shown to increase circulating levels of FGF21 and a moderate decreased body weight due to a reduction in lean body mass while fat mass was increased (Fig. 4E in [41]). Krievina et al. showed that accumulation of adipose tissue in the renal sinus is associated with the visceral adipose amount and increased circulating FGF21 (Table 3 of [40]).

How might FGF21 regulate adipose mass? A previous study showed that FGF21 stimulates both PPARγ expression [83] and PPARγ transcriptional activity by inhibiting sumoylation of the latter [44]. However a subsequent study could not reproduce the finding that FGF21 inhibits PPARγ sumoylation [84]. It has been proposed that the discrepancy between those two studies may be due to different *Fgf21*$^{-/-}$ strains [85]. Therefore, it remains elusive how PPARγ mediates the effects of FGF21. Our findings indicate increased PPARγ expression and reduced SUMO-PPARγ in WAT in HFD-fed *αMHC-KLF5*$^{-/-}$ mice, which are in accordance with increased adiposity.

Our data demonstrate a role for cardiomyocyte KLF5 in regulating body weight. The mechanism via which KLF5 regulates cardiac *Fgf21* expression and whether increased FGF21 levels mediate the effects of MED13 in adiposity remain to be elucidated. In this study, we demonstrate that KLF5 inhibition promotes DIO via a distinct effect of cardiomyocyte FGF21. Moreover, we have uncovered a specific pathway leading from the heart to regulation of body and show that

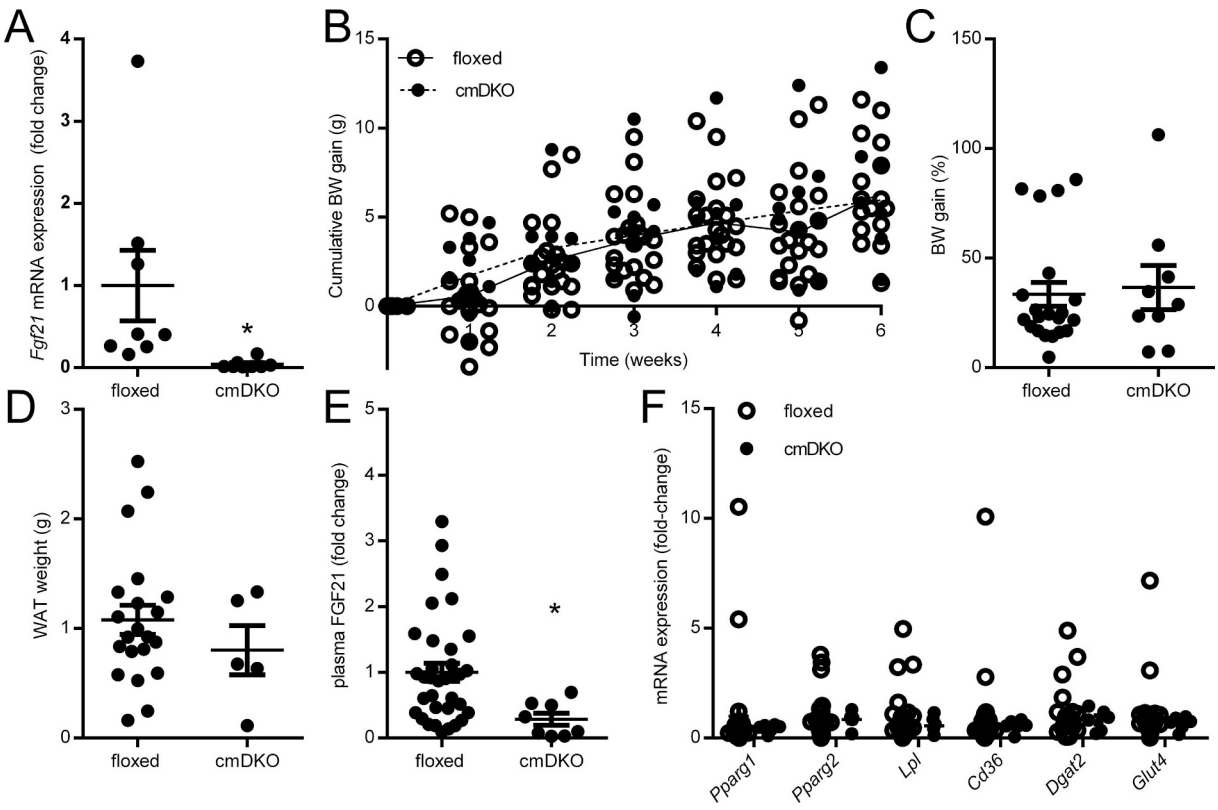

Fig. 7. Cardiomyocyte FGF21 is associated with increased weight gain of HFD-fed αMHC-KLF5$^{-/-}$ mice – A: Cardiac *Fgf21* mRNA levels in control floxed and *αMHC-[KLF5$^{-/-}$;FGF21$^{-/-}$]* mice (n = 8, *p < 0.05 vs floxed with Student's *t*-test). B–D: Cumulative body weight gain (B), body weight gain (C), and posterior subcutaneous WAT weight (D) of control floxed (n = 21) and *αMHC-[KLF5$^{-/-}$;FGF21$^{-/-}$]* (B and C: n = 9, D: n = 5) mice after 6 weeks on HFD. E: Plasma FGF21 levels in control floxed (n = 34; 95% CI 102.4–225.2 pg/ml), and *αMHC-[KLF5$^{-/-}$;FGF21$^{-/-}$]* (n = 8; 95% CI 1.0–115.4 pg/ml) mice after 6 weeks HFD (*p < 0.05 vs floxed with Student's *t*-test). F: mRNA levels of lipid metabolism markers *Pparg1*, *Pparg2*, *Lpl*, *Cd36*, *Dgat2* and *Glut4* in WAT obtained from control floxed (n = 25) and *αMHC-[KLF5$^{-/-}$;FGF21$^{-/-}$]* (n = 6) mice. Data are presented as mean ± SEM. cmDKO is *αMHC-[KLF5$^{-/-}$;FGF21$^{-/-}$]*. Dgat: diglyceride acyltransferase, Glut: glucose transporter, HFD: high fat diet, KLF: Krüppel-like factor, Lpl: lipoprotein lipase, WAT: white adipose tissue. (See also Figs. S1E–G, and S3).

KLF5 is involved in a complex metabolic network that controls WAT development and body weight gain. Overall, our data show a novel hormonally regulated inter-organ cross talk between the heart and systemic metabolism.

Supplementary data to this article can be found online at https://doi.org/10.1016/j.dummy.2019.01.002.

Transparency document

The Transparency document associated this article can be found, in online version.

Acknowledgements

We would like to thank Mesele C. Valenti for technical assistance. The graphical abstract was produced using Servier Medical Art (http://www.servier.com).

Author contributions

Conceptualization K.D., C.J.P.; Methodology, K.D., C.J.P., N.M.P., M.J.J., E.Z., I.D.K., P.N.; Validation, C.J.P., N.M.P.; Formal Analysis, C.J.P., N.M.P., M.J.J., E.Z., I.D.K., I.K.; Investigation, C.J.P, N.M.P., M.J.J., E.Z., I.K., I.D.K., D.A.S, B.R.B., and K.D.; Resources, K.D., I.J.G., G.I.S., I.A.; Writing – Original Draft, C.J.P., K.D.; Writing – Review & Editing, C.J.P., N.M.P., M.J.J., E.Z., I.K., I.D.K., P.N., I.A., G.I.S., I.J.G., K.D.; Supervision K.D.; Project administration, C.J.P., K.D.; Funding Acquisition, K.D, I.J.G., I.A., P.N.

Funding

This work was supported by NHLBI "Pathway to Independence" K99/R00 award HL112853 (K.D.), HL130218 (K.D.), HL45095 and HL73029 (I.J.G.), the W. W. Smith Charitable Trust (K.D.), the FWF project DK-MCD W1226 of the Austrian Science Fund [Fonds zur Förderung der wissenschaftlichen Forschung (FWF)] (N.M.P.), the National Cancer Institute (R00CA188293-02), the American Society of Hematology, the Leukemia Research Foundation, the St. Baldrick's

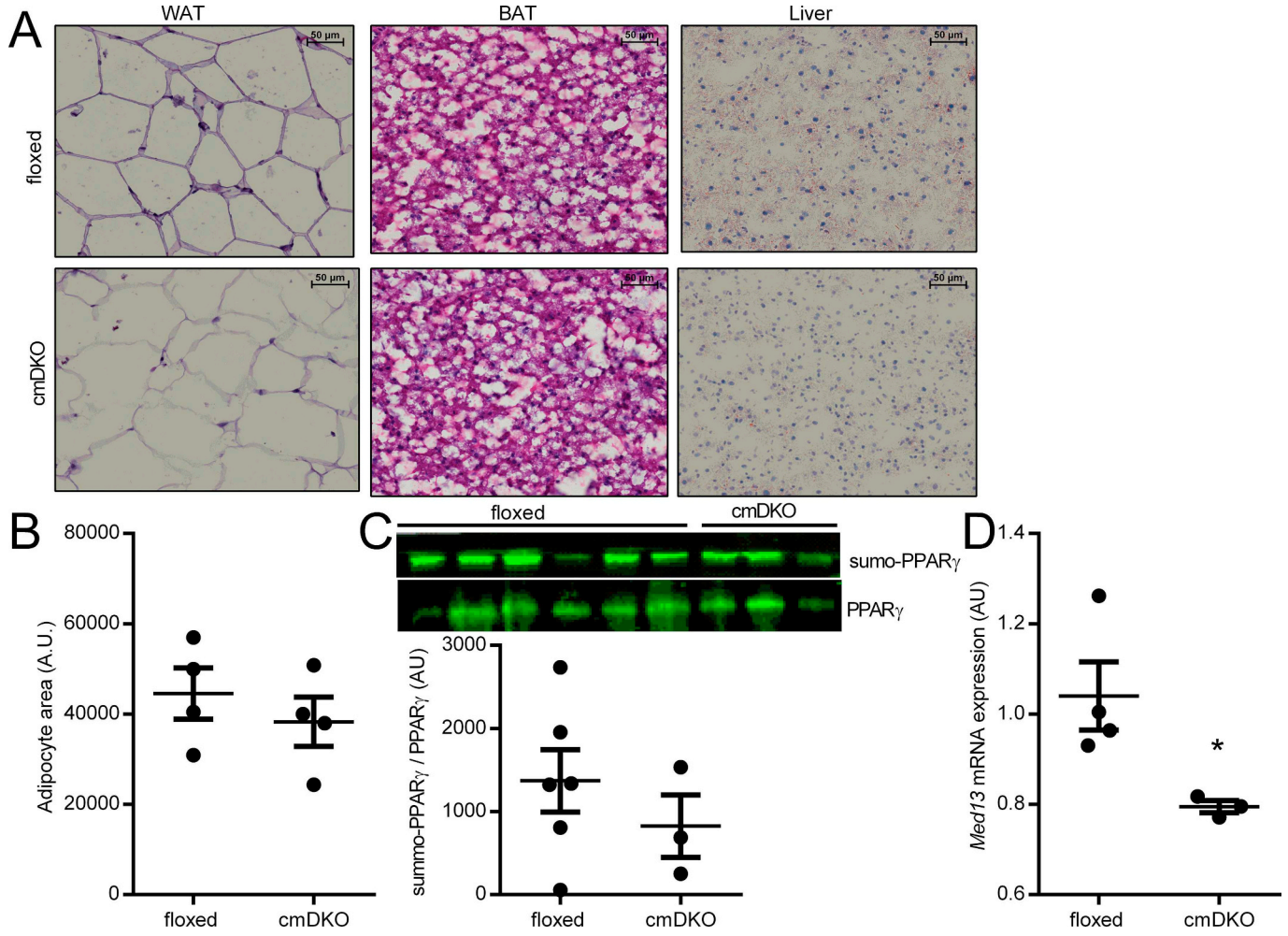

Fig. 8. Cardiomyocyte FGF21 ablation negates the proadipogenic effect of KLF5 deletion – A: Representative pictures of H&E staining of WAT and BAT, and Oil Red O staining of liver of control floxed and *αMHC-[KLF5$^{-/-}$;FGF21$^{-/-}$]* mice after 6 weeks HFD. B: Quantification of WAT adipocyte size (n = 4) of control floxed and *αMHC-[KLF5$^{-/-}$;FGF21$^{-/-}$]* mice after 6 weeks HFD. C: Western Blotting analysis for sumo-PPARγ and PPARγ protein levels obtained with immunoprecipitation from WAT isolated from control floxed and *αMHC-[KLF5$^{-/-}$;FGF21$^{-/-}$]* mice after 6 weeks in HFD (n = 3–6). D: Cardiac *Med13* mRNA levels in HFD-fed control floxed and *αMHC-[KLF5$^{-/-}$;FGF21$^{-/-}$]* mice (n = 4, *$p < 0.05$ vs floxed with Student's *t*-test). Data are presented as mean ± SEM. cmDKO is *αMHC-[KLF5$^{-/-}$;FGF21$^{-/-}$]*. BAT: brown adipose tissue, HFD: high fat diet, KLF: Krüppel-like factor, WAT: white adipose tissue.

Foundation, and the Zell Foundation (P.N.), the "Stavros Niarchos Foundation"-RTP-CEM fellowship by the World Hellenic Biomedical Association-WHBA (E.Z.), the American Heart Association and the Kahn Family Post-Doctoral Fellowship in Cardiovascular Research 18POST34060150 (I.D.K.), the William Lawrence and Blanche Hughes Foundation, the Leukemia & Lymphoma Society, the Ralph S. French Charitable Foundation Trust, the Chemotherapy Foundation, the V Foundation for Cancer Research, the St. Baldrick's Foundation (I.A.). I.A. is a Howard Hughes Medical Institute Early Career Scientist.

References

[1] P.C. Schulze, K. Drosatos, I.J. Goldberg, Lipid use and misuse by the heart, Circ. Res. 118 (2016) 1736–1751.
[2] A. Augustus, H. Yagyu, G. Haemmerle, A. Bensadoun, R.K. Vikramadithyan, S.Y. Park, J.K. Kim, R. Zechner, I.J. Goldberg, Cardiac-specific knock-out of lipoprotein lipase alters plasma lipoprotein triglyceride metabolism and cardiac gene expression, J. Biol. Chem. 279 (2004) 25050–25057.
[3] T. Ogawa, A.J. de Bold, The heart as an endocrine organ, Endocr Connect 3 (2014) R31–R44.
[4] C. Sengenes, M. Berlan, I. De Glisezinski, M. Lafontan, J. Galitzky, Natriuretic peptides: a new lipolytic pathway in human adipocytes, FASEB J. 14 (2000) 1345–1351.
[5] A.L. Birkenfeld, M. Boschmann, C. Moro, F. Adams, K. Heusser, G. Franke, M. Berlan, F.C. Luft, M. Lafontan, J. Jordan, Lipid mobilization with physiological atrial natriuretic peptide concentrations in humans, J. Clin. Endocrinol. Metab. 90 (2005) 3622–3628.
[6] O. Tsukamoto, M. Fujita, M. Kato, S. Yamazaki, Y. Asano, A. Ogai, H. Okazaki, M. Asai, Y. Nagamachi, N. Maeda, et al., Natriuretic peptides enhance the production of adiponectin in human adipocytes and in patients with chronic heart failure, J. Am. Coll. Cardiol. 53 (2009) 2070–2077.
[7] M. Bordicchia, D. Liu, E.Z. Amri, G. Ailhaud, P. Dessi-Fulgheri, C. Zhang, N. Takahashi, R. Sarzani, S. Collins, Cardiac natriuretic peptides act via p38 MAPK to induce the brown fat thermogenic program in mouse and human adipocytes, J. Clin. Invest. 122 (2012) 1022–1036.
[8] J.A. Magida, L.A. Leinwand, Metabolic crosstalk between the heart and liver impacts familial hypertrophic cardiomyopathy, EMBO Mol. Med. 6 (2014) 482–495.
[9] S. Hernandez-Anzaldo, E. Berry, V. Brglez, D. Leung, T.J. Yun, J.S. Lee, J.G. Filep, Z. Kassiri, C. Cheong, G. Lambeau, et al., Identification of a novel heart-liver axis: matrix metalloproteinase-2 negatively regulates cardiac secreted phospholipase A2 to modulate lipid metabolism and inflammation in the liver, J. Am. Heart Assoc. 4 (2015).
[10] K.K. Baskin, C.E. Grueter, C.M. Kusminski, W.L. Holland, A.L. Bookout, S. Satapati, Y.M. Kong, S.C. Burgess, C.R. Malloy, P.E. Scherer, et al., MED13-dependent signaling from the heart confers leanness by enhancing metabolism in adipose tissue and liver, EMBO Mol. Med. 6 (2014) 1610–1621.
[11] C.E. Grueter, E. van Rooij, B.A. Johnson, S.M. DeLeon, L.B. Sutherland, X. Qi, L. Gautron, J.K. Elmquist, R. Bassel-Duby, E.N. Olson, A cardiac microRNA governs systemic energy homeostasis by regulation of MED13, Cell 149 (2012) 671–683.
[12] M.T. Knuesel, K.D. Meyer, C. Bernecky, D.J. Taatjes, The human CDK8 subcomplex is a molecular switch that controls mediator coactivator function, Genes Dev. 23 (2009) 439–451.
[13] P. Tontonoz, B.M. Spiegelman, Fat and beyond: the diverse biology of PPARgamma, Annu. Rev. Biochem. 77 (2008) 289–312.
[14] J. Rieusset, F. Andreelli, D. Auboeuf, M. Roques, P. Vallier, J.P. Riou, J. Auwerx, M. Laville, H. Vidal, Insulin acutely regulates the expression of the peroxisome

proliferator-activated receptor-gamma in human adipocytes, Diabetes 48 (1999) 699–705.
[15] S. Jain, S. Pulikuri, Y. Zhu, C. Qi, Y.S. Kanwar, A.V. Yeldandi, M.S. Rao, J.K. Reddy, Differential expression of the peroxisome proliferator-activated receptor gamma (PPARgamma) and its coactivators steroid receptor coactivator-1 and PPAR-binding protein PBP in the brown fat, urinary bladder, colon, and breast of the mouse, Am. J. Pathol. 153 (1998) 349–354.
[16] B. Desvergne, W. Wahli, Peroxisome proliferator-activated receptors: nuclear control of metabolism, Endocr. Rev. 20 (1999) 649–688.
[17] S.A. Kliewer, K. Umesono, D.J. Noonan, R.A. Heyman, R.M. Evans, Convergence of 9-cis retinoic acid and peroxisome proliferator signalling pathways through heterodimer formation of their receptors, Nature 358 (1992) 771–774.
[18] Z.E. Floyd, J.M. Stephens, Controlling a master switch of adipocyte development and insulin sensitivity: covalent modifications of PPARgamma, Biochim. Biophys. Acta 1822 (2012) 1090–1095.
[19] T. Nishimura, Y. Nakatake, M. Konishi, N. Itoh, Identification of a novel FGF, FGF-21, preferentially expressed in the liver, Biochim. Biophys. Acta 1492 (2000) 203–206.
[20] E.S. Muise, B. Azzolina, D.W. Kuo, M. El-Sherbeini, Y. Tan, X. Yuan, J. Mu, J.R. Thompson, J.P. Berger, K.K. Wong, Adipose fibroblast growth factor 21 is up-regulated by peroxisome proliferator-activated receptor gamma and altered metabolic states, Mol. Pharmacol. 74 (2008) 403–412.
[21] H. Wang, L. Qiang, S.R. Farmer, Identification of a domain within peroxisome proliferator-activated receptor gamma regulating expression of a group of genes containing fibroblast growth factor 21 that are selectively repressed by SIRT1 in adipocytes, Mol. Cell. Biol. 28 (2008) 188–200.
[22] E. Hondares, R. Iglesias, A. Giralt, F.J. Gonzalez, M. Giralt, T. Mampel, F. Villarroya, Thermogenic activation induces FGF21 expression and release in brown adipose tissue, J. Biol. Chem. 286 (2011) 12983–12990.
[23] K. Fon Tacer, A.L. Bookout, X. Ding, H. Kurosu, G.B. John, L. Wang, R. Goetz, M. Mohammadi, M. Kuro-o, D.J. Mangelsdorf, et al., Research resource: comprehensive expression atlas of the fibroblast growth factor system in adult mouse, Mol. Endocrinol. 24 (2010) 2050–2064.
[24] Y. Izumiya, H.A. Bina, N. Ouchi, Y. Akasaki, A. Kharitonenkov, K. Walsh, FGF21 is an Akt-regulated myokine, FEBS Lett. 582 (2008) 3805–3810.
[25] D.R. Crooks, T.G. Natarajan, S.Y. Jeong, C. Chen, S.Y. Park, H. Huang, M.C. Ghosh, W.H. Tong, R.G. Haller, C. Wu, et al., Elevated FGF21 secretion, PGC-1alpha and ketogenic enzyme expression are hallmarks of iron-sulfur cluster depletion in human skeletal muscle, Hum. Mol. Genet. 23 (2014) 24–39.
[26] G. Singhal, F.M. Fisher, M.J. Chee, T.G. Tan, A. El Ouaamari, A.C. Adams, R. Najarian, R.N. Kulkarni, C. Benoist, J.S. Flier, et al., Fibroblast growth factor 21 (FGF21) protects against high fat diet induced inflammation and islet hyperplasia in pancreas, PLoS One 11 (2016) e0148252.
[27] K.C. Coate, G. Hernandez, C.A. Thorne, S. Sun, T.D.V. Le, K. Vale, S.A. Kliewer, D.J. Mangelsdorf, FGF21 is an exocrine pancreas secretagogue, Cell Metab. 25 (2017) 472–480.
[28] A. Planavila, I. Redondo, E. Hondares, M. Vinciguerra, C. Munts, R. Iglesias, L.A. Gabrielli, M. Sitges, M. Giralt, M. van Bilsen, et al., Fibroblast growth factor 21 protects against cardiac hypertrophy in mice, Nat. Commun. 4 (2013) 2019.
[29] V. Patel, R. Adya, J. Chen, M. Ramanjaneya, M.F. Bari, S.K. Bhudia, E.W. Hillhouse, B.K. Tan, H.S. Randeva, Novel insights into the cardio-protective effects of FGF21 in lean and obese rat hearts, PLoS One 9 (2014) e87102.
[30] X. Ding, J. Boney-Montoya, B.M. Owen, A.L. Bookout, K.C. Coate, D.J. Mangelsdorf, S.A. Kliewer, betaKlotho is required for fibroblast growth factor 21 effects on growth and metabolism, Cell Metab. 16 (2012) 387–393.
[31] A.C. Adams, C.C. Cheng, T. Coskun, A. Kharitonenkov, FGF21 requires betaklotho to act in vivo, PLoS One 7 (2012) e49977.
[32] T. Inagaki, P. Dutchak, G. Zhao, X. Ding, L. Gautron, V. Parameswara, Y. Li, R. Goetz, M. Mohammadi, V. Esser, et al., Endocrine regulation of the fasting response by PPARalpha-mediated induction of fibroblast growth factor 21, Cell Metab. 5 (2007) 415–425.
[33] M.K. Badman, P. Pissios, A.R. Kennedy, G. Koukos, J.S. Flier, E. Maratos-Flier, Hepatic fibroblast growth factor 21 is regulated by PPARalpha and is a key mediator of hepatic lipid metabolism in ketotic states, Cell Metab. 5 (2007) 426–437.
[34] F.M. Fisher, S. Kleiner, N. Douris, E.C. Fox, R.J. Mepani, F. Verdeguer, J. Wu, A. Kharitonenkov, J.S. Flier, E. Maratos-Flier, et al., FGF21 regulates PGC-1alpha and browning of white adipose tissues in adaptive thermogenesis, Genes Dev. 26 (2012) 271–281.
[35] F.M. Fisher, P.C. Chui, P.J. Antonellis, H.A. Bina, A. Kharitonenkov, J.S. Flier, E. Maratos-Flier, Obesity is a fibroblast growth factor 21 (FGF21)-resistant state, Diabetes 59 (2010) 2781–2789.
[36] L. Geng, B. Liao, L. Jin, Z. Huang, C.R. Triggle, H. Ding, J. Zhang, Y. Huang, Z. Lin, A. Xu, Exercise alleviates obesity-induced metabolic dysfunction via enhancing FGF21 sensitivity in adipose tissues, Cell Rep. 26 (2019) 2738–2752 e2734.
[37] A. Kharitonenkov, T.L. Shiyanova, A. Koester, A.M. Ford, R. Micanovic, E.J. Galbreath, G.E. Sandusky, L.J. Hammond, J.S. Moyers, R.A. Owens, et al., FGF-21 as a novel metabolic regulator, J. Clin. Invest. 115 (2005) 1627–1635.
[38] T. Coskun, H.A. Bina, M.A. Schneider, J.D. Dunbar, C.C. Hu, Y. Chen, D.E. Moller, A. Kharitonenkov, Fibroblast growth factor 21 corrects obesity in mice, Endocrinology 149 (2008) 6018–6027.
[39] G. Gaich, J.Y. Chien, H. Fu, L.C. Glass, M.A. Deeg, W.L. Holland, A. Kharitonenkov, T. Bumol, H.K. Schilske, D.E. Moller, The effects of LY2405319, an FGF21 analog, in obese human subjects with type 2 diabetes, Cell Metab. 18 (2013) 333–340.
[40] G. Krievina, P. Tretjakovs, I. Skuja, V. Silina, L. Keisa, D. Krievina, G. Bahs, Ectopic adipose tissue storage in the left and the right renal sinus is asymmetric and associated with serum kidney injury molecule-1 and fibroblast growth factor-21 levels increase, EBioMedicine 13 (2016) 274–283.
[41] M.K. Brahma, R.C. Adam, N.M. Pollak, D. Jaeger, K.A. Zierler, N. Pocher, R. Schreiber, M. Romauch, T. Moustafa, S. Eder, et al., Fibroblast growth factor 21 is induced upon cardiac stress and alters cardiac lipid homeostasis, J. Lipid Res. 55 (2014) 2229–2241.
[42] P. Arner, A. Pettersson, P.J. Mitchell, J.D. Dunbar, A. Kharitonenkov, M. Ryden, FGF21 attenuates lipolysis in human adipocytes - a possible link to improved insulin sensitivity, FEBS Lett. 582 (2008) 1725–1730.
[43] X. Li, H. Ge, J. Weiszmann, R. Hecht, Y.S. Li, M.M. Veniant, J. Xu, X. Wu, R. Lindberg, Y. Li, Inhibition of lipolysis may contribute to the acute regulation of plasma FFA and glucose by FGF21 in ob/ob mice, FEBS Lett. 583 (2009) 3230–3234.
[44] P.A. Dutchak, T. Katafuchi, A.L. Bookout, J.H. Choi, R.T. Yu, D.J. Mangelsdorf, S.A. Kliewer, Fibroblast growth factor-21 regulates PPARgamma activity and the antidiabetic actions of thiazolidinediones, Cell 148 (2012) 556–567.
[45] S.S. Chung, B.Y. Ahn, M. Kim, J.H. Kho, H.S. Jung, K.S. Park, SUMO modification selectively regulates transcriptional activity of peroxisome-proliferator-activated receptor gamma in C2C12 myotubes, Biochem. J. 433 (2011) 155–161.
[46] L. Mikkonen, J. Hirvonen, O.A. Janne, SUMO-1 regulates body weight and adipogenesis via PPARgamma in male and female mice, Endocrinology 154 (2013) 698–708.
[47] K. Drosatos, N.M. Pollak, C.J. Pol, P. Ntziachristos, F. Willecke, M.C. Valenti, C.M. Trent, Y. Hu, S. Guo, I. Aifantis, et al., Cardiac myocyte KLF5 regulates Ppara expression and cardiac function, Circ. Res. 118 (2016) 241–253.
[48] Y. Oishi, I. Manabe, K. Tobe, M. Ohsugi, T. Kubota, K. Fujiu, K. Maemura, N. Kubota, T. Kadowaki, R. Nagai, SUMOylation of Kruppel-like transcription factor 5 acts as a molecular switch in transcriptional programs of lipid metabolism involving PPAR-delta, Nat. Med. 14 (2008) 656–666.
[49] W.C. Claycomb, N.A. Lanson Jr., B.S. Stallworth, D.B. Egeland, J.B. Delcarpio, A. Bahinski, N.J. Izzo Jr., HL-1 cells: a cardiac muscle cell line that contracts and retains phenotypic characteristics of the adult cardiomyocyte, Proc. Natl. Acad. Sci. U. S. A. 95 (1998) 2979–2984.
[50] Raake, P.W., Zhang, X., Vinge, L.E., Brinks, H., Gao, E., Jaleel, N., Li, Y., Tang, M., Most, P., Dorn, G.W., 2nd, et al. 2012. Cardiac G-protein-coupled receptor kinase 2 ablation induces a novel Ca2+ handling phenotype resistant to adverse alterations and remodeling after myocardial infarction. Circulation 125:2108–2118.
[51] M.J. Jurczak, A.H. Lee, F.R. Jornayvaz, H.Y. Lee, A.L. Birkenfeld, B.A. Guigni, M. Kahn, V.T. Samuel, L.H. Glimcher, G.I. Shulman, Dissociation of inositol-requiring enzyme (IRE1alpha)-mediated c-Jun N-terminal kinase activation from hepatic insulin resistance in conditional X-box-binding protein-1 (XBP1) knock-out mice, J. Biol. Chem. 287 (2012) 2558–2567.
[52] K. Drosatos, Z. Drosatos-Tampakaki, R. Khan, S. Homma, P.C. Schulze, V.I. Zannis, I.J. Goldberg, Inhibition of c-Jun-N-terminal kinase increases cardiac peroxisome proliferator-activated receptor alpha expression and fatty acid oxidation and prevents lipopolysaccharide-induced heart dysfunction, J. Biol. Chem. 286 (2011) 36331–36339.
[53] H.Q. Zheng, Z. Zhou, J. Huang, L. Chaudhury, J.T. Dong, C. Chen, Kruppel-like factor 5 promotes breast cell proliferation partially through upregulating the transcription of fibroblast growth factor binding protein 1, Oncogene 28 (2009) 3702–3713.
[54] K. Drosatos, R.S. Khan, C.M. Trent, H. Jiang, N.H. Son, W.S. Blaner, S. Homma, P.C. Schulze, I.J. Goldberg, Peroxisome proliferator-activated receptor-gamma activation prevents sepsis-related cardiac dysfunction and mortality in mice, Circ. Heart Fail. 6 (2013) 550–562.
[55] H.L. Noh, K. Okajima, J.D. Molkentin, S. Homma, I.J. Goldberg, Acute lipoprotein lipase deletion in adult mice leads to dyslipidemia and cardiac dysfunction, Am. J. Physiol. Endocrinol. Metab. 291 (2006) E755–E760.
[56] W. Wu, F. Shi, D. Liu, R.P. Ceddia, R. Gaffin, W. Wei, H. Fang, E.D. Lewandowski, S. Collins, Enhancing natriuretic peptide signaling in adipose tissue, but not in muscle, protects against diet-induced obesity and insulin resistance, Sci. Signal. 10 (2017).
[57] S.R. Das, M.H. Drazner, D.L. Dries, G.L. Vega, H.G. Stanek, S.M. Abdullah, R.M. Canham, A.K. Chung, D. Leonard, F.H. Wians Jr.et al., Impact of body mass and body composition on circulating levels of natriuretic peptides: results from the Dallas Heart Study, Circulation 112 (2005) 2163–2168.
[58] T.J. Wang, M.G. Larson, D. Levy, E.J. Benjamin, E.P. Leip, P.W. Wilson, R.S. Vasan, Impact of obesity on plasma natriuretic peptide levels, Circulation 109 (2004) 594–600.
[59] A.M. Khan, S. Cheng, M. Magnusson, M.G. Larson, C. Newton-Cheh, E.L. McCabe, A.D. Coviello, J.C. Florez, C.S. Fox, D. Levy, et al., Cardiac natriuretic peptides, obesity, and insulin resistance: evidence from two community-based studies, J. Clin. Endocrinol. Metab. 96 (2011) 3242–3249.
[60] A.M. Hennige, H. Staiger, C. Wicke, F. Machicao, A. Fritsche, H.U. Haring, N. Stefan, Fetuin-a induces cytokine expression and suppresses adiponectin production, PLoS One 3 (2008) e1765.
[61] R.O. Pereira, S.M. Tadinada, F.M. Zasadny, K.J. Oliveira, K.M.P. Pires, A. Olvera, J. Jeffers, R. Souvenir, R. McGlauflin, A. Seei, et al., OPA1 deficiency promotes secretion of FGF21 from muscle that prevents obesity and insulin resistance, EMBO J. 36 (2017) 2126–2145.
[62] B. Zhou, H. Li, L. Xu, W. Zang, S. Wu, H. Sun, Osteocalcin reverses endoplasmic reticulum stress and improves impaired insulin sensitivity secondary to diet-induced obesity through nuclear factor-kappaB signaling pathway, Endocrinology 154 (2013) 1055–1068.
[63] S. Wang, X. Yang, Inter-organ regulation of adipose tissue browning. Cellular and molecular life sciences, CMLS 74 (2017) 1765–1776.
[64] A. Rodriguez, S. Becerril, S. Ezquerro, L. Mendez-Gimenez, G. Fruhbeck, Crosstalk

between adipokines and myokines in fat browning, Acta Physiol. (Oxford) 219 (2017) 362–381.
[65] K. Ostrowski, T. Rohde, M. Zacho, S. Asp, B.K. Pedersen, Evidence that interleukin-6 is produced in human skeletal muscle during prolonged running, J. Physiol. 508 (1998) 949–953 Pt 3.
[66] N. Suarez-Zamorano, S. Fabbiano, C. Chevalier, O. Stojanovic, D.J. Colin, A. Stevanovic, C. Veyrat-Durebex, V. Tarallo, D. Rigo, S. Germain, et al., Microbiota depletion promotes browning of white adipose tissue and reduces obesity, Nat. Med. 21 (2015) 1497–1501.
[67] K.H. Kim, Y.T. Jeong, H. Oh, S.H. Kim, J.M. Cho, Y.N. Kim, S.S. Kim, D.H. Kim, K.Y. Hur, H.K. Kim, et al., Autophagy deficiency leads to protection from obesity and insulin resistance by inducing Fgf21 as a mitokine, Nat. Med. 19 (2013) 83–92.
[68] J.H. Lee, R. Bassel-Duby, E.N. Olson, Heart- and muscle-derived signaling system dependent on MED13 and Wingless controls obesity in Drosophila, Proc. Natl. Acad. Sci. U. S. A. 111 (2014) 9491–9496.
[69] S. Lee, H. Bao, Z. Ishikawa, W. Wang, H.Y. Lim, Cardiomyocyte regulation of systemic lipid metabolism by the apolipoprotein B-containing lipoproteins in drosophila, PLoS Genet. 13 (2017) e1006555.
[70] S.Y. Park, Y.R. Cho, B.N. Finck, H.J. Kim, T. Higashimori, E.G. Hong, M.K. Lee, C. Danton, S. Deshmukh, G.W. Cline, et al., Cardiac-specific overexpression of peroxisome proliferator-activated receptor-alpha causes insulin resistance in heart and liver, Diabetes 54 (2005) 2514–2524.
[71] K.R. Markan, M.C. Naber, M.K. Ameka, M.D. Anderegg, D.J. Mangelsdorf, S.A. Kliewer, M. Mohammadi, M.J. Potthoff, Circulating FGF21 is liver derived and enhances glucose uptake during refeeding and overfeeding, Diabetes 63 (2014) 4057–4063.
[72] S.A. Dogan, C. Pujol, P. Maiti, A. Kukat, S. Wang, S. Hermans, K. Senft, R. Wibom, E.I. Rugarli, A. Trifunovic, Tissue-specific loss of DARS2 activates stress responses independently of respiratory chain deficiency in the heart, Cell Metab. 19 (2014) 458–469.
[73] L.D. BonDurant, M. Ameka, M.C. Naber, K.R. Markan, S.O. Idiga, M.R. Acevedo, S.A. Walsh, D.M. Ornitz, M.J. Potthoff, FGF21 regulates metabolism through adipose-dependent and -independent mechanisms, Cell Metab. 25 (2017) 935–944 e934.
[74] A.C. Adams, C. Yang, T. Coskun, C.C. Cheng, R.E. Gimeno, Y. Luo, A. Kharitonenkov, The breadth of FGF21's metabolic actions are governed by FGFR1 in adipose tissue, Molecular metabolism 2 (2012) 31–37.
[75] Z. Lin, H. Tian, K.S. Lam, S. Lin, R.C. Hoo, M. Konishi, N. Itoh, Y. Wang, S.R. Bornstein, A. Xu, et al., Adiponectin mediates the metabolic effects of FGF21 on glucose homeostasis and insulin sensitivity in mice, Cell Metab. 17 (2013) 779–789.
[76] W.L. Holland, A.C. Adams, J.T. Brozinick, H.H. Bui, Y. Miyauchi, C.M. Kusminski, S.M. Bauer, M. Wade, E. Singhal, C.C. Cheng, et al., An FGF21-adiponectin-ceramide axis controls energy expenditure and insulin action in mice, Cell Metab. 17 (2013) 790–797.
[77] R.J. Samms, C.C. Cheng, A. Kharitonenkov, R.E. Gimeno, A.C. Adams, Overexpression of beta-klotho in adipose tissue sensitizes male mice to endogenous FGF21 and provides protection from diet-induced obesity, Endocrinology 157 (2016) 1467–1480.
[78] S. Talukdar, Y. Zhou, D. Li, M. Rossulek, J. Dong, V. Somayaji, Y. Weng, R. Clark, A. Lanba, B.M. Owen, et al., A long-acting FGF21 molecule, PF-05231023, decreases body weight and improves lipid profile in non-human primates and type 2 diabetic subjects, Cell Metab. 23 (2016) 427–440.
[79] J. Xu, D.J. Lloyd, C. Hale, S. Stanislaus, M. Chen, G. Sivits, S. Vonderfecht, R. Hecht, Y.S. Li, R.A. Lindberg, et al., Fibroblast growth factor 21 reverses hepatic steatosis, increases energy expenditure, and improves insulin sensitivity in diet-induced obese mice, Diabetes 58 (2009) 250–259.
[80] M.K. Badman, A. Koester, J.S. Flier, A. Kharitonenkov, E. Maratos-Flier, Fibroblast growth factor 21-deficient mice demonstrate impaired adaptation to ketosis, Endocrinology 150 (2009) 4931–4940.
[81] T. Lan, D.A. Morgan, K. Rahmouni, J. Sonoda, X. Fu, S.C. Burgess, W.L. Holland, S.A. Kliewer, D.J. Mangelsdorf, FGF19, FGF21, and an FGFR1/beta-klotho-activating antibody act on the nervous system to regulate body weight and glycemia, Cell Metab. 26 (2017) 709–718 e703.
[82] D.J. Klemm, J.W. Leitner, P. Watson, A. Nesterova, J.E. Reusch, M.L. Goalstone, B. Draznin, Insulin-induced adipocyte differentiation. Activation of CREB rescues adipogenesis from the arrest caused by inhibition of prenylation, J. Biol. Chem. 276 (2001) 28430–28435.
[83] J.S. Moyers, T.L. Shiyanova, F. Mehrbod, J.D. Dunbar, T.W. Noblitt, K.A. Otto, A. Reifel-Miller, A. Kharitonenkov, Molecular determinants of FGF-21 activity-synergy and cross-talk with PPARgamma signaling, J. Cell. Physiol. 210 (2007) 1–6.
[84] A.C. Adams, T. Coskun, C.C. Cheng, O.F. LS, S.L. Dubois, A. Kharitonenkov, Fibroblast growth factor 21 is not required for the antidiabetic actions of the thiazoladinediones, Mol Metab 2 (2013) 205–214.
[85] F.M. Fisher, E. Maratos-Flier, SUMO wars, Mol Metab 3 (2014) 81–83.